ACS OMEGA

http://pubs.acs.org/journal/acsodf

Article

Influence of the Injection Scheme on the Enhanced Oil Recovery Ability of Heterogeneous Phase Combination Flooding in Mature Waterflooded Reservoirs

Wenzheng Liu, Hong He,* Fuqing Yuan, Haocheng Liu, Fangjian Zhao, Huan Liu, and Guangjie Luo

Cite This: *ACS Omega* 2022, 7, 23511−23520

Read Online

ACCESS | Metrics & More | Article Recommendations

ABSTRACT: With the maturity of waterflooded reservoirs, owing to serious heterogeneity, the fluid will channel through the thief zone, leading to considerable remaining oil unrecovered in the upswept area. To further enhance oil recovery (EOR) after waterflooding, the heterogeneous phase combination flooding (HPCF) was composed of a polymer, branched-preformed particle gel (B-PPG), and surfactant. For the sake of improving the economic efficiency, the influence of the injection scheme on the EOR of HPCF with an equal chemical agent cost was investigated by sand-pack flooding experiments. Then, visual plate sand-pack model flooding experiments were performed to study the swept area of HPCF under different injection schemes. Results demonstrated that the total EOR of HPCF under different injection schemes ranged from 33.5 to 39.3%. Moreover, the EOR of HPCF under the alternation injection (AI) scheme was the highest, followed by the concentration step change injection (CI) scheme, and that of the simultaneous injection (SI) scheme was the least. The visual flooding experimental results showed that the swept area of HPCF after waterflooding under the AI scheme was higher than that of the SI. Moreover, in view of qualitative analysis of remaining oil distribution, the EOR of AI of HPCF was higher than that of SI, which was consistent with the parallel sand-pack flooding results.

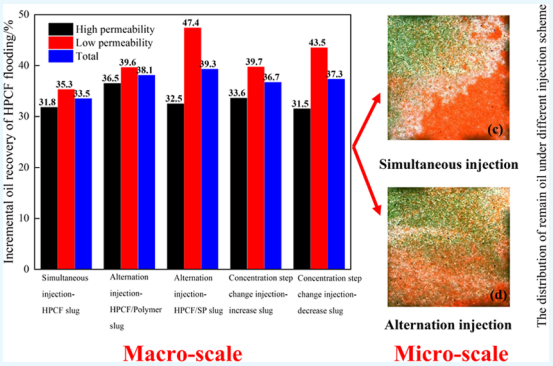

1. INTRODUCTION

After the primary oil recovery relying on formation energy, waterflooding as a secondary oil recovery technology has been applied to maintain formation energy to improve oil recovery.[1,2] However, with the maturity of waterflooded reservoirs, owing to serious heterogeneity, the water will enter through the dominant percolation channels and lead to inefficient or even ineffective circulation,[3] which results in considerable remaining oil unrecovered on the upswept area and low waterflooding recovery.[4] Moreover, due to the adverse oil−water viscosity ratio and high oil−water interfacial tension, the swept volume and oil displacement efficiency of waterflooding are worse.[5] Previous research shows that about 70% remaining oil exists in nonmain streamline areas and not effectively swept.[6] Therefore, improving the swept volume and oil displacement efficiency of injected water is the major method to enhance the recovery of remaining oil.[7] Based on the technological innovation and field application, it is confirmed that chemical flooding technology is able to substantially enhance oil recovery of the mature reservoir.[8,9] Related technologies include polymer flooding,[10−13] surfactant flooding,[14−17] alkali-free binary compound flooding,[18−20] foam flooding,[21−24] etc. Currently, nanoparticles have been used as additives in the polymer, surfactant, and foam for further improving oil recovery by changing the wettability, reducing the interfacial tension, and improving the mobility ratio.[25,26] These technologies have been applied in many oilfields and achieved significant economic benefits.[27] Among these chemical flooding technologies, polymer flooding has been widely applied in mature waterflooded reservoirs.[28] The high viscosity of the polymer solution can reduce the oil−water mobility ratio and inhibit the fingering phenomenon during the displacement process.[28−30] Nevertheless, for serious heterogeneous mature reservoirs, the viscous polymer can have limited ability of expanding the swept volume.

Polymer gels have been commonly used for conformance control or water shutoff treatment in seriously heterogeneous mature reservoirs, which can have better ability of expanding the swept volume.[31,32] Polymer gels can be further divided into in situ polymer gels and preformed particle gels (PPG).[6] In situ polymer gels with a three-dimensional network structure are formed by the crosslinking reaction of a polymer and a

Received: April 1, 2022
Accepted: June 10, 2022
Published: June 28, 2022

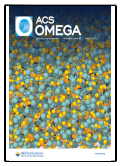

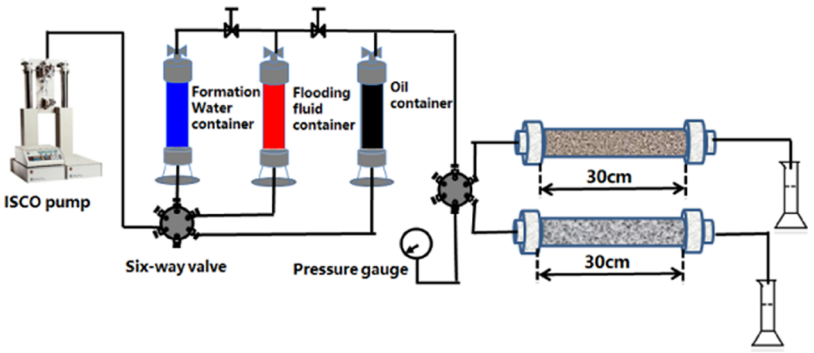

Figure 1. Schematic diagram of the experimental apparatus.

crosslinking agent. Nevertheless, there are many factors that affect the crosslinking reaction and gelation performance, leading to the uncertainty of gelation and uncontrollable gelation time.[33,34] Therefore, to overcome the problem of the uncertainty of gelation, preformed particle gels have been developed and attracted extensive attention in recent years. PPGs can absorb water and swell to form soft solid particles.[35] Based on the mechanism of migration, plugging, and deformation, the sweep efficiency can be improved remarkably.[36−38] On this basis, the branched-preformed particle gel (B-PPG) has been developed by introducing linear branched chains into the main chain of PPG molecules. The linear branched chains can be soluble in water and play a role in increasing the viscosity, which improves the suspension ability of particles.[39]

Aiming at the goal of expanding the swept volume and improving the displacement efficiency, a heterogeneous phase combination flooding system (HPCF) composed of the polymer, surfactant, and B-PPG was proposed.[4,40−42] The synergistic effect of homogeneous polymer−surfactant and heterogeneous B-PPG on the EOR was investigated in previous study. Moreover, a field pilot test of HPCF has been implemented in the Zhongyiqu Ng3 block, Gudao oil plant of the Shengli oilfield. The results of the field pilot test showed that the total daily oil production increased from 4.5 to 81.2 t/d, and the comprehensive water cut was decreased by 18.5% and oil recovery was increased by 3.5%.[43] So far, the HPCF technology has been applied on a large scale in SINOPEC. It is estimated that the covered reserves will reach 1.5×10^8 t.[44]

In recent years, some scholars have found that the EOR efficiency of chemical flooding can be improved by changing the injection schemes of chemical agents. In addition, a reasonable injection scheme can reduce the amount of the chemical agent for the purpose of ensuring oil recovery. Nevertheless, previously reported research has been mainly focused on the chemical flooding injection scheme of traditional oil displacement agents such as polymers and focused less on HPCF.[45−47] Moreover, previous studies mainly focused on numerical simulation investigation and lacked relevant laboratory physical simulation experiments. In addition, it is not enough to elucidate the displacement mechanism of HPCF with different injection methods from the core scale.

Therefore, the aim of this study is to analyze the displacement efficiency and mechanism of HPCF under different injection schemes through macroscale and microscale flooding experiments. Thus, first, the influence of the injection scheme on the enhanced oil recovery ability of HPCF with an equal chemical agent cost was investigated by a series of parallel sand-pack flooding from the macroscale level. The injection schemes were optimized according to the fractional flow and incremental oil recovery. Then, the visual plate sand-pack heterogeneous model (15 cm × 15 cm × 6 mm) displacement experiments were conducted to directly observe the flooding behavior of HPCF from the microscale level. According to the qualitative analysis of remaining oil distribution, the incremental oil recoveries under injection schemes were calculated. Finally, we hope that these results in this study can better guide the promotion of HPCF and the high-efficiency development of mature reservoirs.

2. EXPERIMENTAL SECTION

2.1. Materials. The B-PPG with an elastic modulus of 10.3 Pa used in the experiments was provided by Sinopec of China, and the diameter of B-PPG after swelling in the formation water was measured using a Bettersize 2600. It could be found by observing the appearance of B-PPG before and after swelling that because B-PPG goes through the crushing process after crosslinking on the ground, the shape of B-PPG is not a regular sphere after swelling. HPAM used in this study with a molecular mass of 2.0×10^7 was provided by SNF. The surfactant is a nonionic surfactant provided by the Shengli oilfield. The total dissolved solids (TDS) of simulated formation brine were 21190.35 mg·L^{-1}, including 7466.15 mg·L^{-1} Na^+, 428 mg·L^{-1} Ca^{2+}, 255.7 mg·L^{-1} Mg^{2+}, and 13040.5 mg·L^{-1} Cl^{-1}. The experimental oil was dehydrated crude oil obtained from the Shengtuo oilfield, and its viscosity was 76 mPa·s at 80 °C.

2.2. Methods. *2.2.1. Measurement of Particle Size Distribution Characteristics.* The particle size distribution of B-PPG after swelling was determined using a Bettersize 2600 laser particle size analyzer following the procedures: (1) The B-PPG suspension was obtained by adding a determined amount of dry powder into the simulated formation brine under the stirring rate of 300 r·min^{-1} for 2.0 h. (2) Then, the particle size distribution characteristic and the D_{50} of B-PPG was measured.

2.2.2. Parallel Sand-Pack Test. The influence of the injection scheme on the EOR ability of HPCF was investigated by flooding experiments. The schematic diagram of the experimental apparatus is plotted in Figure 1. The size of the sand pack was Φ2.5 cm × 30 cm. The experimental procedures are as follows: (1) Sand packing: Different-permeability sand packs were obtained using the wet-packing method. During the filling process, quartz sand and simulation formation brine were alternately added and compacted. (2) Oil saturation period: crude oil flooding was conducted to obtain irreducible water saturation at the flow rate of 0.1 mL/min. (3) Aging: the oil-saturated sand pack was put into an oven and aged at 80 °C for 48 h to restore the reservoir wettability. (4) Waterflooding period: Waterflooding was conducted at the flow rate of 0.5 mL/

https://doi.org/10.1021/acsomega.2c02007
ACS Omega 2022, 7, 23511−23520

Table 1. Scheme of the Slug Design

injection scheme	chemical slug[a]	chemical formulation
simultaneous injection	HPCF	0.3 PV(0.16%P + 0.08%B-PPG + 0.3%S)
alternation injection	HPCF/P	0.228 PV(0.16%P + 0.08%B-PPG + 0.3%S)+0.228 PV(0.16%P)
	HPCF/SP	0.168 PV(0.16%P + 0.08%B-PPG + 0.3%S) + 0.168 PV(0.16%P + 0.3%S)
concentration step increase injection	HPCF	0.1 PV(0.12%P + 0.06%B-PPG + 0.3%S) + 0.1 PV(0.16%P + 0.08%B-PPG + 0.3%S) + 0.1 PV(0.20%P + 0.10%B-PPG + 0.3%S)
concentration step decrease injection	HPCF	0.1 PV(0.20%P + 0.10%B-PPG + 0.3%S) + 0.1 PV(0.16%P + 0.08%B-PPG + 0.3%S) + 0.1 PV(0.12%P + 0.06%B-PPG + 0.3%S)

[a]All the main slugs with the equivalent economical cost.

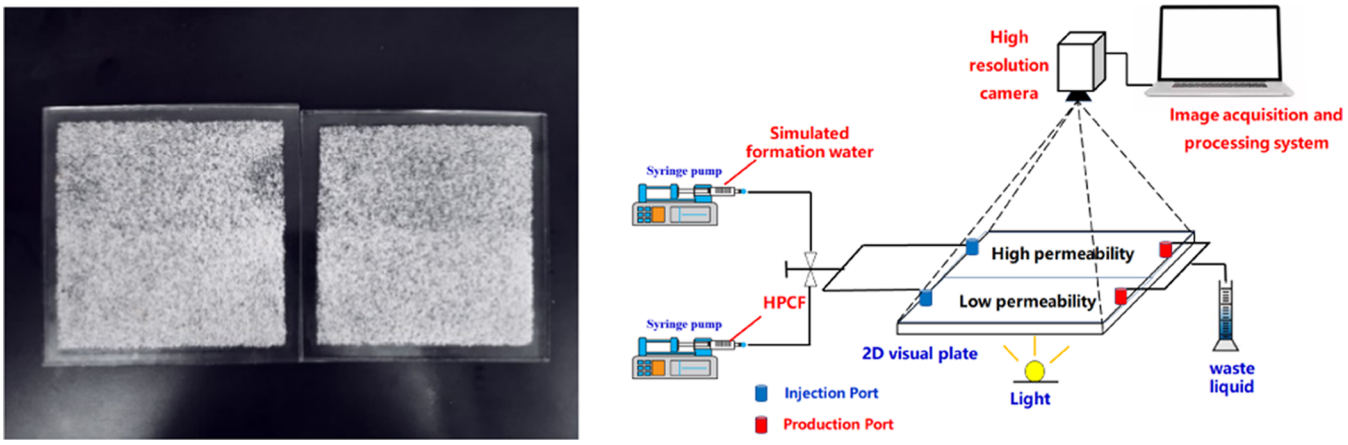

Figure 2. Appearance of the visual plate sand model and sketch map of the experimental apparatus.

Table 2. Design of Visual Experiments under Different Injection Schemes

injection scheme	injection rate mL/min	chemical slug	chemical formulation
simultaneous injection	0.5	HPCF	0.3 PV(0.16%P + 0.08%B-PPG + 0.3%S)
alternation injection		HPCF/SP	0.168 PV(0.16%P + 0.08%B-PPG + 0.3%S) + 0.168 PV(0.16%P + 0.3%S)

min. Waterflooding was terminated when the water cut reached 95%. (5) HPCF period: different HPFC slugs were injected under different injection schemes, and then, extended waterflooding was implemented until the overall water cut reached 98%. The experimental scheme design is shown in Table 1.

2.2.3. Visual Experiment. The visual plate sand-pack model flooding experiments were conducted to illustrate the mechanism of HPCF enlarging the swept volume with different injection schemes. The experimental apparatus includes a syringe pump, visual plate sand model (15 cm × 15 cm, and 6 mm in depth), LED light source. Figure 2 shows the sketch map of the experimental apparatus.

The simulated oil was prepared using kerosene and paraffin oil in the ratio of 1:3. The viscosity of simulated oil was 23.2 mPa·s at ambient temperature. To more clearly observe the oil−water distribution during the experiment, methyl green was used to dye the HPCF, and Sudan III was used to dye the oil. The scheme of the experiment is shown in Table 2.

The injection rate of the visual test was 0.5 mL/min. The specific steps of visual plate sand model flooding experiments are as follows: (1) the model was vacuumized for 5 h and saturated with water; (2) the simulated oil was pumped into the plate until no water was produced; (3) initial waterflooding was implemented until the water cut reached 95%; (5) HPCF under different injection schemes was conducted; and (6) subsequent waterflooding was conducted until the water cut reached 98%.

3. RESULTS AND DISCUSSION

3.1. Property Evaluation of the HPCF Suspension.

3.1.1. Size Distribution of B-PPG Particles. Figure 3 shows the size distribution of B-PPG with different mass concentrations. When the concentration ranges from 600 to 1000 mg·L^{-1}, the particle size distribution of B-PPG is almost consistent and

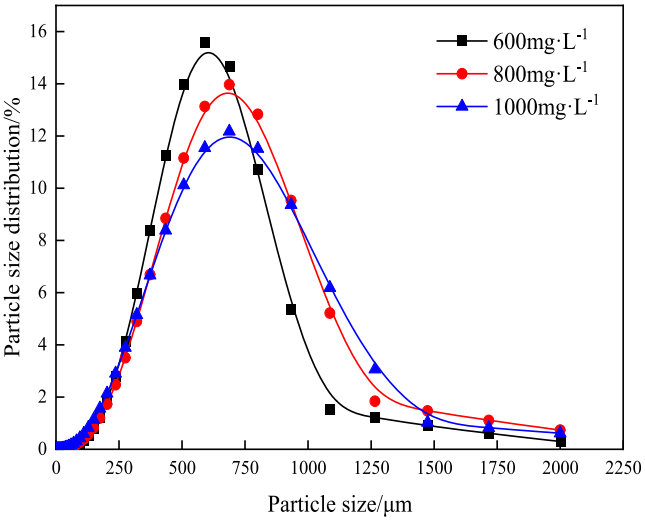

Figure 3. Size distribution of B-PPG versus mass concentration.

https://doi.org/10.1021/acsomega.2c02007
ACS Omega 2022, 7, 23511−23520

mainly distributed in the range from 228.7 to 1474.0 μm. The median diameter of D_{50} is in the range from 506.5 to 550.2 μm, which indicates that the particle size of B-PPG is less affected by the suspension concentration.

3.1.2. Viscosity of the Polymer, B-PPG, and HPCF. The viscosity values of the polymer solution, B-PPG suspension, and HPCF system were measured at reservoir temperature, as shown in Figure 4.

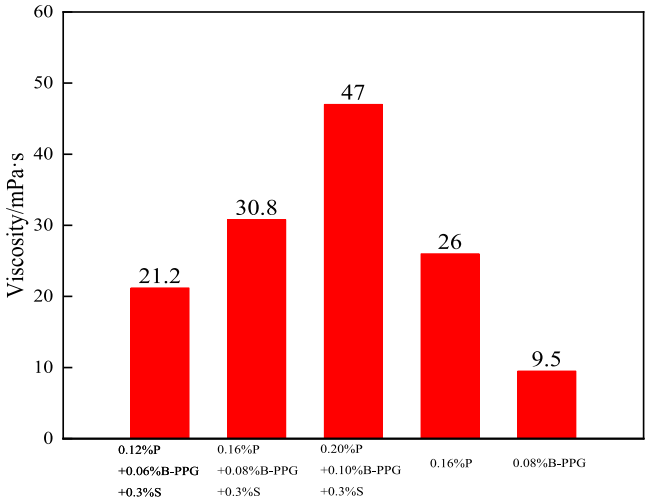

Figure 4. Viscosity of the polymer, B-PPG, and HPCF system.

Compared with the viscosity of B-PPG or the polymer, the viscosity of the HPCF suspension is higher. After adding B-PPG to the polymer solution, the viscosity of the system increases from 26.0 to 30.8 mPa·s. It indicates that B-PPG has a certain viscosity increasing effect. Moreover, with the increase of the polymer and B-PPG concentration in the HPCF system, the viscosity of the suspension increases.

3.2. Parallel Sand-Pack Experimental Results. HPCF is an innovative oil displacement agent, which was composed of a polymer, B-PPG, and surfactant. Therefore, HPCF has the advantages that the traditional tertiary oil recovery method does not have. In this study, the EOR ability of HPCF under simultaneous injection (SI), alternation injection (AI), and concentration step change injection (CI) was analyzed. The basic parameters of the core are shown in Table 3.

3.2.1. Fractional Flow Analysis. The curves of fractional flows can directly reflect the flow diversion effect and profile control ability. Figure 5 depicts the curves of fractional flows of HPCF under different injection schemes at different flooding stages

As shown in Figure 5a−e, the results of fractional flow analysis for different injection schemes at each flooding period have some similar change trends. Before implementing HPCF, owing to the permeability ratio, there is a significant difference in the fractional low of two sand packs. The fractional flow ratio of high-permeability and low-permeability areas was 90:10, approximately. This is the dilemma confronted by waterflooding development in heterogeneous reservoirs. As the HPCF was implemented, the fractional flow of low-permeability sand packs increased gradually. At the end of HPCF, the fractional flow was more than 30% in low-permeability sand packs and less than 70% at high permeability in Figure 7C, and the fractional flow ratio of high- and low-permeability sand packs accounts for 50%.

After conducting extended waterflooding, owing to the continuous plugging of HPCF, the fractional flow in low-permeability sand packs was higher than that in high-permeability sand packs. In contrast, when HPCF was injected under AI, the time of keeping an equal fractional flow ratio of high- and low-permeability sand packs was longer than that in other injection schemes. In other words, the heterogeneous reservoir can be adjusted to homogeneous and maintained for a long time when the injection scheme was AI.

3.2.2. Flooding Characteristic Analysis. According to the experimental method in 2.2.2 and simulating the conditions of heterogeneous reservoirs, parallel sand-pack experiments were implemented. For the sake of evaluating the EOR ability of HPCF under different injection schemes, the experimental data of three injection schemes were gathered and analyzed. Thereafter, the results are shown in Figure 6a−e.

It can be found from Figure 6a−e that different injection schemes have some similar change trends. Specifically, during the initial waterflooding period of the five experiments, an extremely short anhydrous oil production stage was experienced. Afterward, the water cut increased sharply until 80%; then, the increasing rate of water cut slowed down. After injecting 1.3 PV simulated formation water approximately, the water cut exceeded 95%; at this time, the overall incremental oil recovery was approximately 39%. It indicated that a stable percolation channel was formed in the high-permeability area. There was still a large amount of remaining oil in the low-permeability area. After implementing HPCF, the curves of oil recovery and water cut indicated that the injection schemes had a significant effect on the EOR in heterogeneous reservoirs after waterflooding; the water cut decreased from 95 to 40%, approximately.

Moreover, the pressure curves also showed a similar change trend. During the initial waterflooding period, with the increase of the injection pore volume, the injection pressure increased first and then decreased after reaching the start-up pressure.

Table 3. Basic Parameters of Sand Packs

injection scheme	chemical slug design	sand packs	permeability (μm^2)	permeability ratio	porosity (%)	S_{oi} (%)
simultaneous injection	HPCF	high permeability	3.25	3.22	39.40	86.21
		low permeability	1.01		38.04	85.71
alternate injection	HPCF/P	high permeability	3.03	3.19	41.40	83.60
		low permeability	0.95		40.70	86.67
	HPCF/SP	high permeability	3.01	2.92	38.36	84.60
		low permeability	1.03		39.40	86.20
concentration step increase injection	HPCF	high permeability	3.12	3.09	39.4	87.71
		low permeability	1.01		38.7	89.11
concentration step decrease injection	HPCF	high permeability	3.25	3.22	39.5	86.2
		low permeability	1.01		38.8	85.7

https://doi.org/10.1021/acsomega.2c02007
ACS Omega 2022, 7, 23511−23520

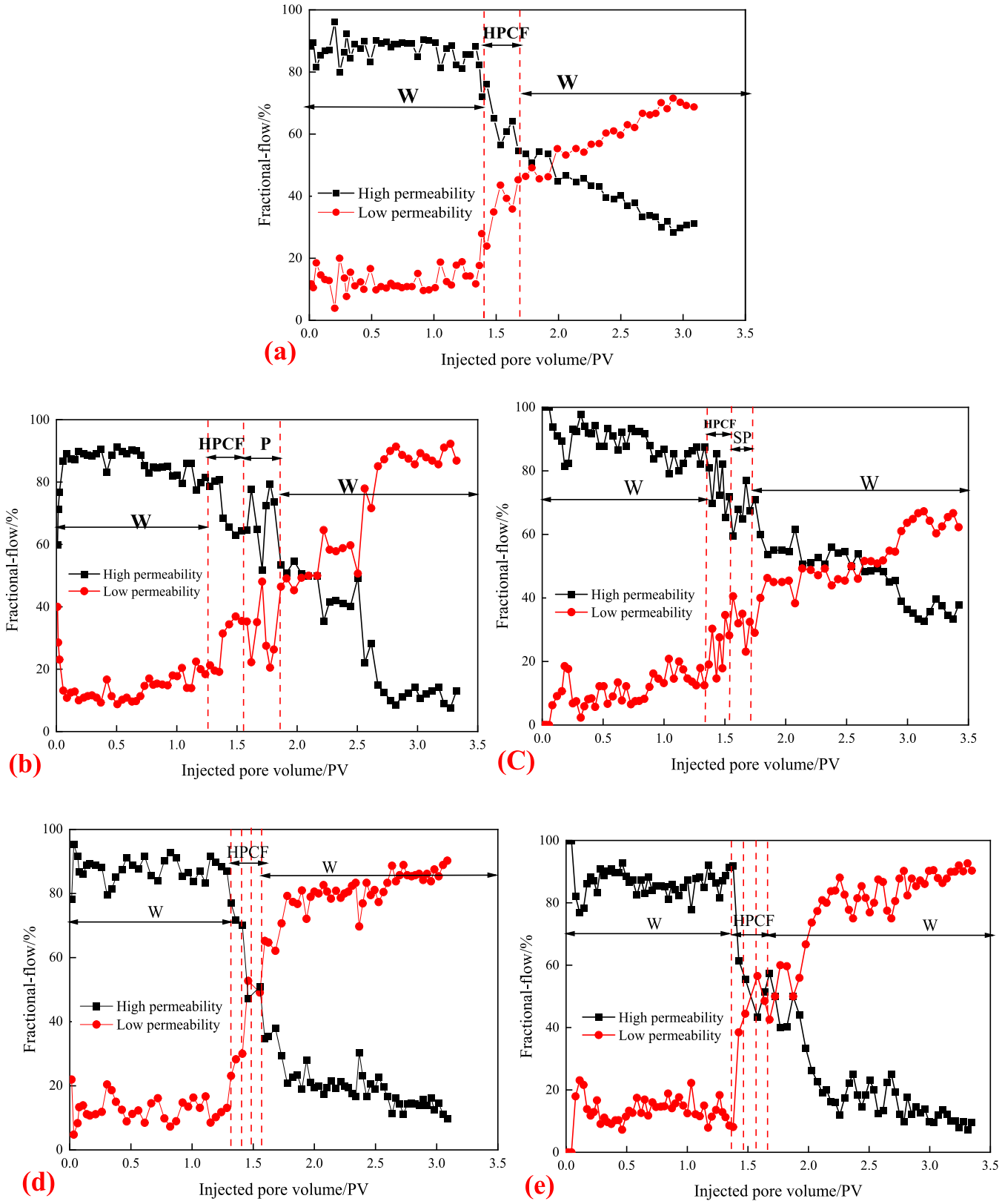

Figure 5. Fractional flows of three injection schemes: (a) SI-HPCF flooding; (b) AI-HPCF/P flooding; (c) AI-HPCF/SP flooding; (d) CI—concentration increase; and (e) CI—concentration decrease.

Thereafter, as the percolation channel was formed, the injection pressure trended toward a stable value. While HPCF was implemented, due to the profile control ability, the percolation resistance of the high-permeability area increased, which resulted in the increase of injection pressure. After implementing subsequent waterflooding, B-PPG could flow in the sand packs by "migration, plugging, deforming, and remigration"; the

https://doi.org/10.1021/acsomega.2c02007
ACS Omega 2022, 7, 23511−23520

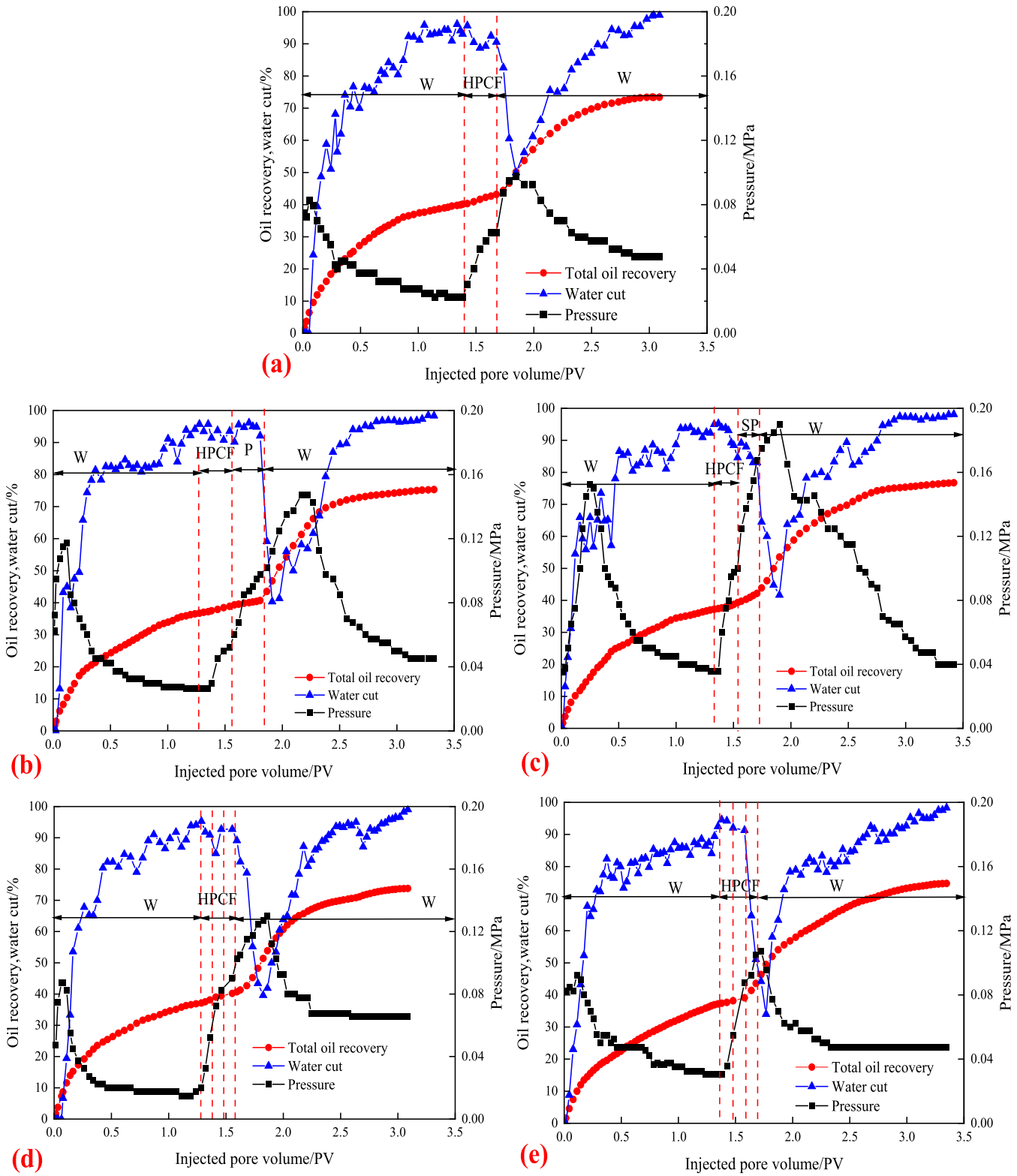

Figure 6. Oil displacement effect curve: (a) SI-HPCF; (b) AI-HPCF/P flooding; (c) AI-HPCF/P flooding; and (d) CI—concentration increase; and (e) CI—concentration decrease.

injection pressure decreased slowly, which prolonged the period of EOR validity.

For the sake of further evaluating the EOR ability of HPCF with different injection schemes, Figure 7 and Table 4 show the results of oil recovery of each period.

It can be found that the oil recovery is mainly contributed by the high-permeability area during the initial waterflooding stage. Owing to the permeability ratio, the injected water penetrated into the high-permeability area, resulting in the stable percolation channel formation, and extensive remaining oil was unswept.

https://doi.org/10.1021/acsomega.2c02007
ACS Omega 2022, 7, 23511−23520

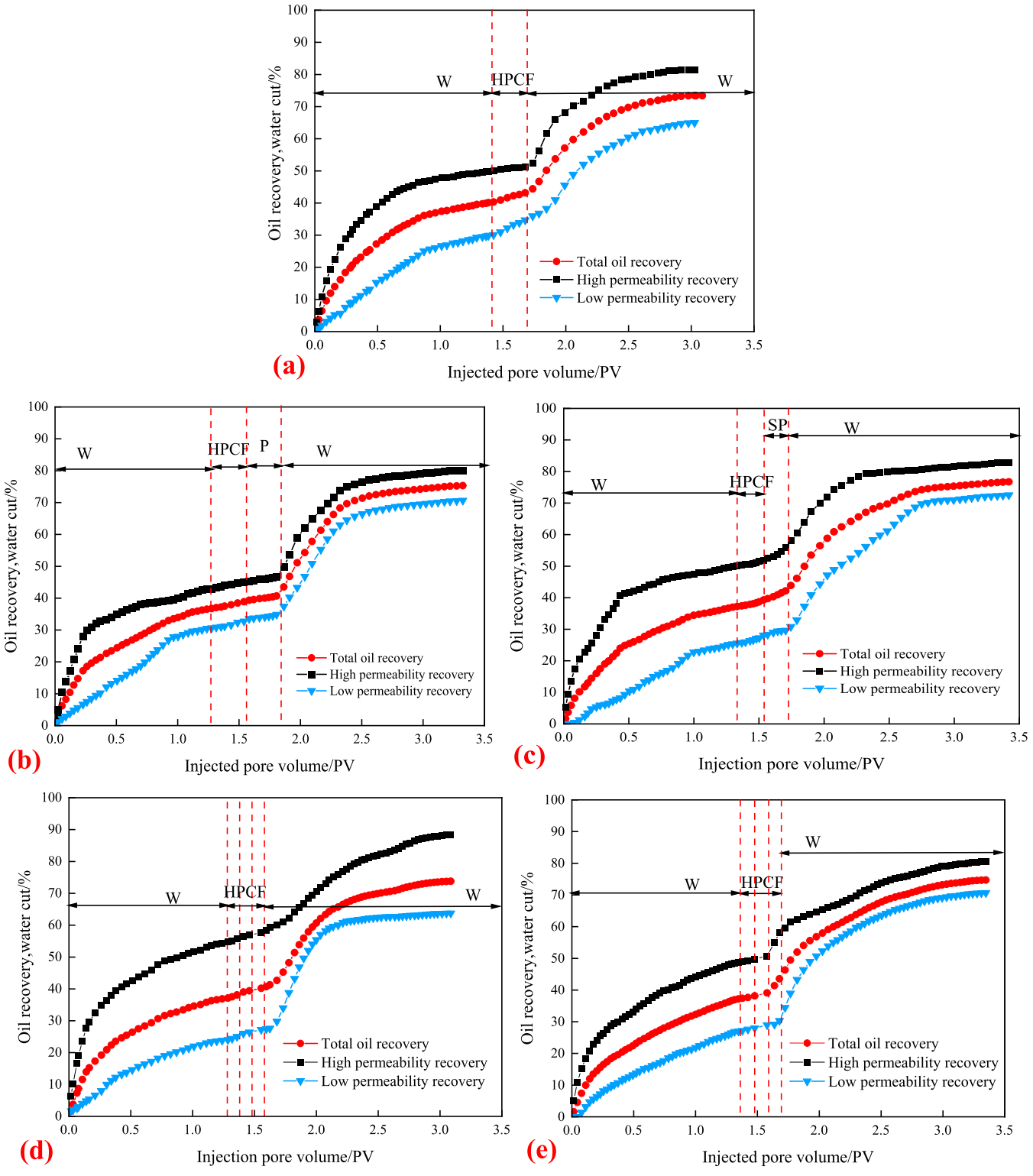

Figure 7. Displacement performance curve: (a) SI-HPCF; (b) AI-HPCF/P flooding; (c) AI-HPCF/P flooding; (d) CI—concentration increase; and (e) CI—concentration decrease.

When HPCF was implemented, the total incremental oil recoveries of HPCF ranged from 33.5 to 39.3%. The experimental dates indicated that HPCF could considerably enhance oil recovery in heterogeneous reservoirs. As can be observed from Figure 8 and Table 4, the enhanced oil recovery ability of AI is the highest, followed by the CI scheme, and the SI scheme has the least ability. Moreover, the oil recovery of AI of the HPCF/SP slug (No. 3) is slightly higher than that of AI of the HPCF/P slug (No. 2). The result can be explained as follows: when the HPCF/SP slug and HPCF/P slug were implemented under the equivalent economic cost, after the HPCF was injected, owing to the increase of the percolation resistance of the high-permeability area, the subsequent SP binary system was diverted into the low-permeability area.

https://doi.org/10.1021/acsomega.2c02007
ACS Omega 2022, 7, 23511−23520

Table 4. Oil Recovery in Different Periods

no.	injection scheme	main slug		enhanced oil recovery(%OOIP) waterflooding	after HPCF flooding	incremental recovery of HPCF flooding
1	simultaneous injection	HPCF	high permeability	49.8	81.6	31.8
			low permeability	29.7	65.0	35.3
			total	39.9	73.4	33.5
2	alternation injection	HPCF/P	high permeability	43.5	80.0	36.5
			low permeability	31.0	70.6	39.6
			total	37.2	75.3	38.1
3		HPCF/SP	high permeability	50.4	82.9	32.5
			low permeability	25.1	72.5	47.4
			total	37.4	76.7	39.3
4	concentration step change injection	concentration increase	high permeability	54.7	88.3	33.6
			low permeability	24.0	63.7	39.7
			total	37.1	73.8	36.7
5		concentration decrease	high permeability	49.1	80.6	31.5
			low permeability	27.2	70.7	43.5
			total	37.4	74.7	37.3

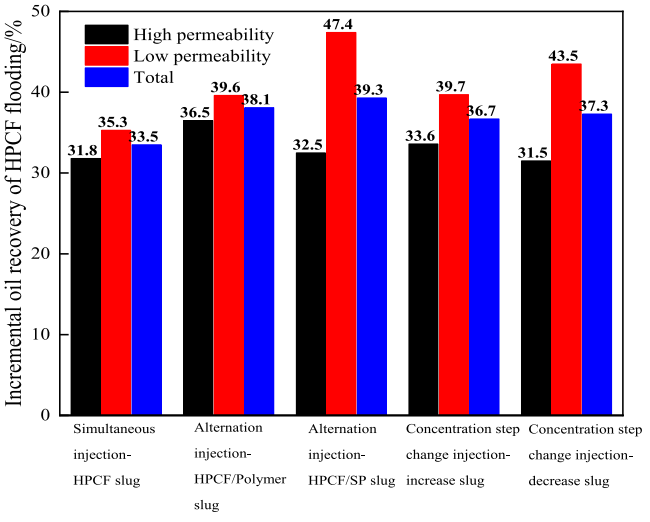

Figure 8. Comparison of oil recovery under different injection schemes.

Considering the effect of sweep efficiency and oil displacement efficiency of the SP binary system, the oil recovery of the low-permeability area was significantly improved.

3.3. Visual Flooding Experimental Results. *3.3.1. Distribution of Remaining Oil.* Figures 9 and 10 show the distribution of remaining oil at different flooding stages under SI and AI schemes, respectively.

Owing to the existence of the permeability ratio and because there was no barricade between high-permeability and low-permeability regions, the main streamline occurred in the high-permeability area, leading to the formation of percolation channels and considerable remaining oil in the both sides of the formed percolation channels. After implementing HPCF, the HPCF system still flowed along the formed percolation channels at the early stage. With the continuous injection of HPCF, the injected liquid was diverted into the low-permeability region and expanded the swept area. Furthermore, it could be found that the swept area of AI of HPCF was higher than that of SI of HPCF. During the subsequent waterflooding period, the HPCF could produce a continuous effect on the plugging and further expanded the sweep area. The capacity of expanding the sweep area of AI was higher than that of SI under the equal economic cost principle.

3.3.2. Analysis of Improve Oil Recovery. Figure 11 shows the incremental oil recovery at each flooding period. According to the visual flooding results, the incremental oil recovery of SI of the HPCF slug and AI of the HPCF/SP slug after waterflooding was 25.4 and 26.2%, respectively. After HPCF was implemented under different injection schemes, the cumulative oil recovery increased by 64.3 and 78.7% OOIP, respectively. The EOR of AI was higher than that of SI, which was consistent with the parallel sand-pack flooding results.

4. CONCLUSIONS

To explore the effect of the injection scheme on the EOR ability of HPCF, parallel sand-pack flooding and visual plate flooding experiments were conducted, and some conclusions could be drawn:

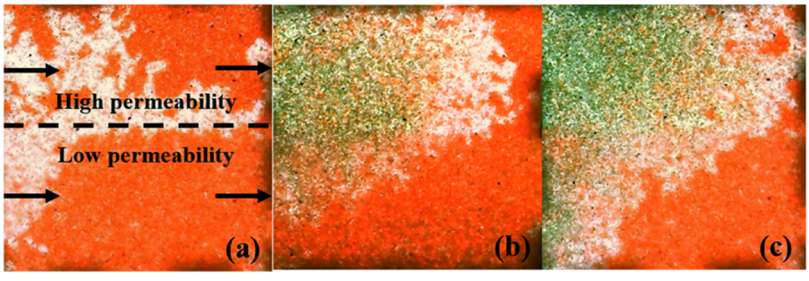

Figure 9. Visual images of simultaneous injection: (a) after waterflooding; (b) after HPCF flooding; and (c) after subsequent waterflooding.

https://doi.org/10.1021/acsomega.2c02007
ACS Omega 2022, 7, 23511−23520

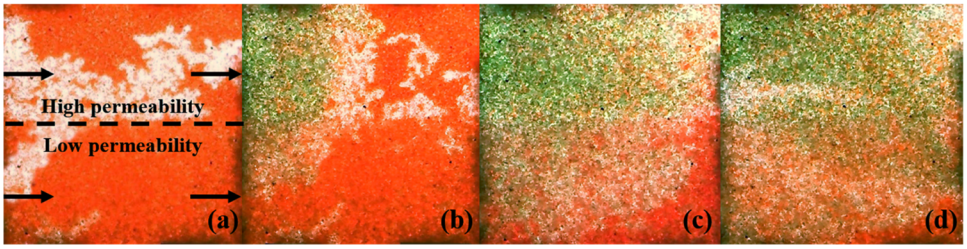

Figure 10. Visual images of alternation injection: (a) waterflooding; (b) HPCF flooding; (c) SP flooding; and (d) subsequent waterflooding.

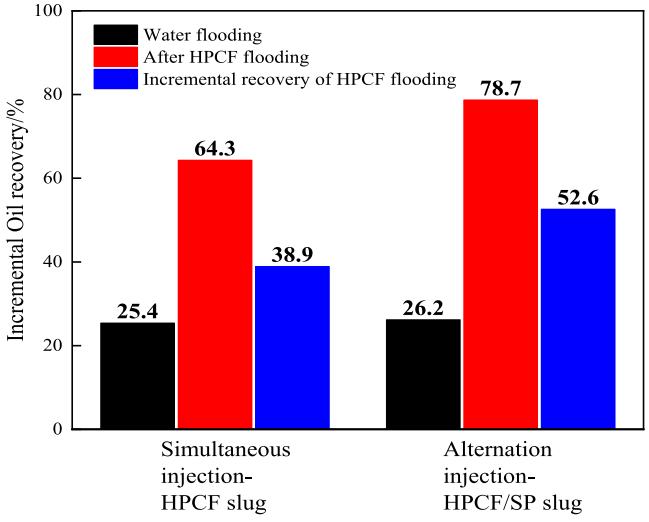

Figure 11. EOR of HPCF under different injection schemes.

(1) The results of parallel sand-pack displacement experiments demonstrated that the EOR of HPCF after waterflooding with different injection schemes ranged from 33.5 to 39.3%, and the low-permeability area enhanced by 35.3−47.4% OOIP. Moreover, the EOR of HPCF under the AI scheme was the highest, followed by the CI scheme, and the SI scheme had the least EOR. Moreover, the EOR of the HPCF/SP slug is higher than that of the HPCF/P slug under the AI scheme.

(2) The visual flooding experimental results showed that the swept area of HPCF after waterflooding under the AI scheme was higher than that of SI. Furthermore, on the basis of qualitative analysis of remaining oil distribution, the EOR of AI of HPCF was higher than that of SI, which was consistent with the parallel sand-pack flooding results.

AUTHOR INFORMATION

Corresponding Author

Hong He − *College of Petroleum Engineering, Yangtze University, Wuhan 430100, China; Key Laboratory of Drilling and Production Engineering for Oil and Gas, Hubei Province, Wuhan 430100, China;* orcid.org/0000-0002-7798-2749; Email: hehong1103@163.com

Authors

Wenzheng Liu − *College of Petroleum Engineering, Yangtze University, Wuhan 430100, China; Key Laboratory of Drilling and Production Engineering for Oil and Gas, Hubei Province, Wuhan 430100, China*

Fuqing Yuan − *Research Institute of Exploration and Development of Shengli Oilfield, SINOPEC, Dongying 257000, China*

Haocheng Liu − *Hekou Oil Production Plant of Shengli Oilfield, Dongying 257000, China*

Fangjian Zhao − *Research Institute of Exploration and Development of Shengli Oilfield, SINOPEC, Dongying 257000, China*

Huan Liu − *College of Petroleum Engineering, Yangtze University, Wuhan 430100, China; Key Laboratory of Drilling and Production Engineering for Oil and Gas, Hubei Province, Wuhan 430100, China*

Guangjie Luo − *College of Petroleum Engineering, Yangtze University, Wuhan 430100, China; Key Laboratory of Drilling and Production Engineering for Oil and Gas, Hubei Province, Wuhan 430100, China*

Complete contact information is available at: https://pubs.acs.org/10.1021/acsomega.2c02007

Notes

The authors declare no competing financial interest.

ACKNOWLEDGMENTS

This work was supported by the National Natural Science Foundation of China (Project Number: 51604037) and the Research Institute of Exploration and Development of the Shengli Oilfield.

REFERENCES

(1) Maroufi, P.; Ayatollahi, S.; Rahmanifard, H.; Jahanmiri, A.; Riazi, M. Experimental investigation of secondary and tertiary oil recovery from fractured porous media. *J. Pet. Explor. Prod. Technol.* **2013**, *3*, 179−188.

(2) Ogbeiwi, P.; Aladeitan, Y.; Udebhulu, D. An approach to waterflood optimization: case study of the reservoir X. *J. Pet. Explor. Prod. Technol.* **2018**, *8*, 271−289.

(3) You, J.; Kyung, L. Pore-Scale Numerical Investigations of the Impact of Mineral Dissolution and Transport on the Heterogeneity of Fracture Systems During CO_2-Enriched Brine Injection. *SPE J.* **2022**, *27*, 1379−1395.

(4) Wu, D.; Zhou, K.; Hou, J.; An, Z.; Zhai, M.; Liu, W. Experimental study on combining heterogeneous phase composite flooding and streamline adjustment to improve oil recovery in heterogeneous reservoirs. *J. Pet. Sci. Eng.* **2020**, *194*, No. 107478.

(5) van Dijke, K.; Kobayashi, I.; Schroën, K.; Uemura, K.; Nakajima, M.; Boom, R. Effect of viscosities of dispersed and continuous phases in microchannel oil-in-water emulsification. *Microfluid. Nanofluid.* **2010**, *9*, 77−85.

(6) Dai, C.; Liu, Y.; Zou, C.; You, Q.; Yang, S.; Zhao, M.; Zhao, G.; Wu, Y.; Sun, Y. Investigation on matching relationship between dispersed particle gel (DPG) and reservoir pore-throats for in-depth profile control. *Fuel* **2017**, *207*, 109−120.

(7) Yang, Z.; Jia, S.; Zhang, L.; Wu, X.; Dou, H.; Guo, Z.; Zeng, L.; Li, H.; Guo, L.; Jia, Z.; Fang, W. Deep profile adjustment and oil displacement sweep control technique for abnormally high temperature and high salinity reservoirs. *Pet. Explor. Dev.* **2016**, *43*, 97−105.

(8) Hou, J.; Zhang, Y.; Lu, N.; Yao, C.; Lei, G. L. A new method for evaluating the injection effect of chemical flooding. *Pet. Sci.* **2016**, *13*, 496−506.
(9) Park, S.; Euy, L.; Sulaiman, W. Adsorption behaviors of surfactants for chemical flooding in enhanced oil recovery. *J. Ind. Eng. Chem.* **2015**, *21*, 1239−1245.
(10) Unsal, E.; Berge, A.; Wever, D. Low salinity polymer flooding: Lower polymer retention and improved injectivity. *J. Pet. Sci. Eng.* **2018**, *163*, 671−682.
(11) Gao, C.; Shi, J.; Zhao, F. Successful polymer flooding and surfactant-polymer flooding projects at Shengli Oilfield from 1992 to 2012. *J. Pet. Explor. Prod. Technol.* **2014**, *4*, 1−8.
(12) Ibiam, E.; Geiger, S.; Almaqbali, A.; Demyanov, V.; Arnold, D. In *Numerical Simulation of Polymer Flooding in a Heterogeneous Reservoir: Constrained versus Unconstrained Optimization*, SPE Nigeria Annual International Conference and Exhibition, SPE-193400-MS, **2018**.
(13) Abedi, B.; Ghazanfari, M.; Kharrat, R. Experimental Study of Polymer Flooding in Fractured Systems Using Five-Spot Glass Micromodel: The Role of Fracture Geometrical Properties. *Energy Explor. Exploit.* **2012**, *30*, 689−705.
(14) Skauge, A.; Garnes, J.; Mørner, O.; Torske, L. Optimization of a surfactant flooding process by core-flood experiments. *J. Pet. Sci. Eng.* **1992**, *7*, 117−130.
(15) Daghlian Sofla, S. J.; Mohammad, S.; Abdolhossein, S. Toward mechanistic understanding of natural surfactant flooding in enhanced oil recovery processes: The role of salinity, surfactant concentration and rock type. *J. Mol. Liq.* **2016**, *222*, 632−639.
(16) Dai, C.; Wang, K.; Liu, Y.; Fang, J.; Zhao, M. Study on the reutilization of clear fracturing flowback fluids in surfactant flooding with additives for Enhanced Oil Recovery (EOR). *PLoS One* **2014**, *9*, No. e113723.
(17) Bai, Y.; Xiong, C.; Shang, X.; Xin, Y. Experimental Study on Ethanolamine/Surfactant Flooding for Enhanced Oil Recovery. *Energy Fuel* **2014**, *28*, 1829−1837.
(18) Li, Y.; Zhang, W.; Shen, Z.; Jin, J.; Su, Z.; Yao, F.; Wang, B.; Yu, X.; Bao, X.; He, X.; Wu, X.; Zhang, H.; Cui, L.; Sha, O. Pilot Test of Surfactant/Polymer Flood with Mixtures of Anionic/Cationic Surfactants for High-Temperature Low-Permeability Sandstone Reservoir. *SPE Reservoir Eval. Eng.* **2021**, *24*, 889−900.
(19) Liu, Z.; Li, Y.; Chen, X.; Chen, Y.; Lyu, J.; Sui, M. The Optimal Initiation Timing of Surfactant-Polymer Flooding in a Waterflooded Conglomerate Reservoir. *SPE J.* **2021**, *26*, 2189−2202.
(20) Hongyan, W.; Cao, X.; Zhang, J.; Zhang, A. Development and application of dilute surfactant−polymer flooding system for Shengli oilfield. *J. Pet. Sci. Eng.* **2009**, *65*, 45−50.
(21) Hosseini-Nasab, S. M.; Douarche, F.; Simjoo, M.; Nabzar, L.; Bourbiaux, B.; Zitha, P. L. J.; Roggero, F. Numerical simulation of foam flooding in porous media in the absence and presence of oleic phase. *Fuel* **2018**, *225*, 655−662.
(22) Zhaoguo, L.; Yan, W.; Zhou, J.; Yuan, Y.; Zeng, S.; Fan, W. Numerical simulation of air−foam flooding in Wuliwan District 1 of Jing'an Oilfield. *J. Pet. Explor. Prod. Technol.* **2019**, *9*, 1531−1538.
(23) Sagir, M.; Mushtaq, M.; Tahir, M. B.; Tahir, M. S.; Ullah, S.; Shahzad, K.; Rashid, U. CO_2 foam for enhanced oil recovery (EOR) applications using low adsorption surfactant structure. *Arabian J. Geosci.* **2018**, *11*, No. 789.
(24) Wang, D.; Hou, Q.; Luo, Y.; Zhu, Y.; Fan, H. Feasibility Studies on CO_2 Foam Flooding EOR Technique After Polymer Flooding for Daqing Reservoirs. *J. Dispersion Sci. Technol.* **2015**, *36*, 453−461.
(25) Cheraghian, G.; Rostami, S.; Afrand, M. Nanotechnology in Enhanced Oil Recovery. *Processes.* **2020**, *8*, 1073.
(26) Cheraghian, G.; Tardasti, S. *Improved Oil Recovery by the Efficiency of Nano-Particle in Imbibition Mechanism*, 2nd EAGE international conference KazGeo, 2012.
(27) Cheraghian, G.; Hendraningrat, L. A review on applications of nanotechnology in the enhanced oil recovery part A: effects of nanoparticles on interfacial tension. *Int Nano Lett.* **2016**, *6*, 129−138.
(28) Zhong, H.; Li, Y.; Zhang, W.; Li, D. Study on microscopic flow mechanism of polymer flooding. *Arabian J. Geosci.* **2019**, *12*, No. 56.
(29) Abdul Hamid, S. A.; Muggeridge, A. H. Analytical solution of polymer slug injection with viscous fingering. *Comput. Geosci.* **2018**, *22*, 711−723.
(30) Husveg, T.; Stokka, M.; Husveg, R.; Stephane, J. The Development of a Low-Shear Valve Suitable for Polymer Flooding. *SPE J.* **2020**, *25*, 2632−2647.
(31) Bai, B.; Zhou, J.; Yin, M. A comprehensive review of polyacrylamide polymer gels for conformance control. *Pet. Explor. Dev.* **2015**, *42*, 525−532.
(32) Zhu, D.; Hou, J.; Wei, Q.; Chen, Y. Development of a High-Temperature-Resistant Polymer-Gel System for Conformance Control in Jidong Oil Field. *SPE Reservoir Eval. Eng.* **2019**, *22*, 100−109.
(33) Leng, J.; Wei, M.; Bai, B. Impact of Polymer Rheology on Gel Treatment Performance of Horizontal Wells with Severe Channeling. *SPE J.* **2022**, *27*, 1017−1035.
(34) Alshehri, A. J.; Wang, J.; Kwak, H. T.; AlSofi, A. M.; Gao, J. A Study of Gel-Based Conformance Control Within Fractured Carbonate Cores Using Low-Field Nuclear-Magnetic-Resonance Techniques. *SPE Reservoir Eval. Eng.* **2019**, *22*, 1063−1074.
(35) Goudarzi, A.; Zhang, H.; Varavei, A.; Taksaudom, P.; Hu, Y.; Delshad, M.; Bai, B.; Sepehrnoori, K. A laboratory and simulation study of preformed particle gels for water conformance control. *Fuel* **2015**, *140*, 502−513.
(36) Imqam, A.; Bai, B. Optimizing the strength and size of preformed particle gels for better conformance control treatment. *Fuel* **2015**, *148*, 178−185.
(37) Farasat, A.; Sefti, M. V.; Sadeghnejad, S.; Saghafi, H. R. Mechanical entrapment analysis of enhanced preformed particle gels (PPGs) in mature reservoirs. *J. Pet. Sci. Eng.* **2017**, *157*, 441−450.
(38) Saghafi, H. R. Retention characteristics of enhanced preformed particle gels (PPGs) in porous media: Conformance control implications. *J. Pet. Sci. Eng.* **2018**, *166*, 962−968.
(39) He, H.; Fu, J.; Hou, B.; Yuan, F.; Guo, L.; Li, Z.; You, Q. Investigation of Injection Strategy of Branched-Preformed Particle Gel/Polymer/Surfactant for Enhanced Oil Recovery after Polymer Flooding in Heterogeneous Reservoirs. *Energies* **2018**, *11*, 1950.
(40) Zhao, G.; Dai, C.; You, Q. Characteristics and displacement mechanisms of the dispersed particle gel soft heterogeneous compound flooding system. *Pet. Explor. Dev.* **2018**, *45*, 481−490.
(41) Gong, H.; Zhang, H.; Xu, L.; Li, K.; Yu, L.; Li, Y.; Dong, M. Further enhanced oil recovery by branched-preformed particle gel/HPAM/surfactant mixed solutions after polymer flooding in parallel-sandpack models. *RSC Adv.* **2017**, *7*, 39564−39575.
(42) Gong, H.; Zhang, H.; Xu, L.; Li, K.; Yu, L.; Qian, S.; Li, Y.; Dong, M. The Synergistic Effect of Branched-Preformed Particle Gel and Hydrolyzed Polyacrylamide on Further-Enhanced Oil Recovery after Polymer Flooding. *Energy Fuels* **2017**, *31*, 7904−7910.
(43) Sun, H. Application of pilot test for well pattern adjusting heterogeneous combination flooding after polymer flooding-case of Zhongyiqu Ng3 block, Gudao oilfield. *Pet. Geol. Recovery Effic.* **2014**, *21*, 1−4.
(44) Sun, H. Development and Opinions of Chemical EOR Technology for High-temperature and High-Salinity Reservoirs. *Pet. Sci. Technol. Forum* **2021**, *40*, 1−7.
(45) Hu, J.; Li, A.; Memon, A. Experimental Investigation of Polymer Enhanced Oil Recovery under Different Injection Modes. *ACS Omega* **2020**, *5*, 31069−31075.
(46) Liu, S.; Shen, A.; Qiu, F.; Liang, S.; Wang, F. Matching Relationship and Alternating Injection for Polymer Flooding in Heterogeneous Formations: A Laboratory Case Study of Daqing Oilfield. *Energies* **2017**, *10*, 1018.
(47) Cao, R.; Yang, H.; Sun, W.; Ma, Y. Z. A new laboratory study on alternate injection of high strength foam and ultra-low interfacial tension foam to enhance oil recovery. *J. Pet. Sci. Eng.* **2015**, *125*, 75−89.

https://doi.org/10.1021/acsomega.2c02007
ACS Omega 2022, 7, 23511−23520